

# Feasibility of MRI-based polymer gel dosimetry using parallel RF transmission with multiple RF source

Sang-Young Kim<sup>1</sup>, Hyeonman Baek<sup>2</sup>, Jung-Hoon Lee<sup>1</sup>, Do-Wan Lee<sup>1</sup>, Jin-Young Jung<sup>1</sup>, and Bo-Young Choe<sup>1</sup>

<sup>1</sup>Department of Biomedical Engineering, The Catholic University of Korea, Seoul, Seoul, Korea, <sup>2</sup>Korea Basic Science Institute, Seoul, Korea

## INTRODUCTION

The polymer gel dosimeter utilizes the mechanism of radiation-induced polymerization of the monomer. When the gel is irradiated, the co-monomers polymerize to crosslinked polyacrylamide, resulting in a change of spin-spin relaxation time,  $T_2$ . It was found that the relaxation rate,  $R_2=1/T_2$ , is proportional to the absorbed dose, making the gel as an interesting 3D dosimetry method. Dose maps are directly derived from  $R_2$  images. However, the inaccuracy and artifacts in the  $R_2$  maps that may result from eddy currents or an inhomogeneous  $B_1$  field can cause severe dose errors. The attempts have been made to reduce deviations of the measured  $R_2$  values [1]. Multiple transmit channels and RF sources can facilitate better control of the RF field and can therefore yield more uniform excitation and homogeneous  $B_1$  field in imaged volume [2]. In this study, we aimed to quantify the inaccuracy in gel dosimetry by comparing conventional single source RF transmit system with MultiTransmit excitation. To evaluate the dose uncertainty in the  $R_2$ -derived dose images, we used the concept of dose resolution proposed by Baldock et al [3]. Furthermore, we assessed the temporal variation in the dose response for MRI-based gel dosimetry.

## MATERIALS AND METHODS

**Polymer gel phantom** The gel was made of BANG<sup>®</sup>3 (MGS research) polymer gel (water + gelatin + methacrylic acid), 1 mole of ascorbic acid-L, and 0.1 mole of  $\text{CuSO}_4$ . The polymer gel was contained in 16 small glass vials (2 cm diameter and 9 cm long cylinder) and a 500 ml plastic phantom (9 cm diameter and 10 cm long). Experiments were repeated over a period of 2 weeks after irradiation to investigate temporal changes in gels.

**Irradiation** The small vials and phantom were irradiated individually using a 6 MV photon beam (Varian Medial System, Palo Alto, CA) in a water bath. The small vials were irradiated to various doses with  $15 \times 15 \text{ cm}^2$  field size (Fig. 1). A 500 ml phantom was irradiated using a pair of 5 cm  $\times$  5 cm parallel opposing lateral beams. **MR imaging** All phantoms were scanned together with 32-channel whole-body 3.0 T MRI system (Achieva 3.0 T TX; Philips) equipped with dual-source parallel RF transmission technology. Multi-slice multi-echo sequence ( $\text{TR}/\Delta\text{TE}=3000/20$  ms, the number of echoes=32,  $\text{FOV}=24 \text{ cm} \times 24 \text{ cm}$ , pixel size= $0.45 \text{ mm} \times 0.45 \text{ mm}$ , slice thickness=3 mm,  $\text{NEX}=1$ ) was used for  $R_2$  measurements. To compare  $B_1$  field in imaged volumes between single and MultiTransmit RF transmission, we used double angle method [4] for  $B_1$  map ( $\text{TR}/\text{TE}=8000/2.4$  ms,  $\text{NEX}=1$ ,  $\alpha_1=45^\circ$ , and  $\alpha_2=90^\circ$ ).

**$R_2$  estimation** The MATLAB program was used to calculate  $R_2$  maps from 32 echoes images using non-linear regression method. The standard uncertainty of  $R_2$  defined by  $\sigma(R_2)$  was also evaluated. **Dose resolution** Dose resolution describes the minimum difference in dose that can be detected at a certain level of confidence  $p$ . For a linear dose response, it is given by:  $D_\Delta = k p \times 2^{1/2} \times \sigma_{R_2} \times 1/a_1$  where  $k_p$  is the value given by the  $t$  distribution for experimental degrees of freedom, e.g.,  $k_{0.95\%}$  is 1.96.

## RESULTS AND DISCUSSION

As shown in Fig.1,  $B_1$  uniformity index on MultiTransmit method were significantly lower than on the conventional single-source image, suggesting the actual flip angles and local signal intensity distribution are more consistent on the MultiTransmit images. Furthermore, it is important to note that  $\sigma(R_2)$  was lower on the MultiTransmit images than on the conventional single-source images (Fig.2 bottom layer). And there was a temporal variation in the  $R_2$  response of BANG3 gel between the scanning sessions (from week to week). In the second measurement (1 week after), slight increases in the  $R_2$  and  $\rho_0$  values were observed compared to the first measurement. Lastly, the MultiTransmit measurement gives a lower  $D_\Delta$  than that obtained using the conventional single-source method (Fig. 3). We found that absolute dosimetry measured using the MultiTransmit MR imaging method is in good general agreement with the calculated dose distribution within the suggested dose tolerance. On the other hand, conventional single-source MR imaging can cause a dose error of up to 12%.

## CONCLUSION

We demonstrated for the first time the feasibility of MultiTransmit MR imaging for introducing gel dosimetry into a clinical routine. The improved image quality and  $B_1$  homogeneity resulted in reduced dose uncertainty (i.e.,  $\sigma(R_2)$ ) and in MRI-based polymer gel dosimetry, suggesting that MultiTransmit MR imaging has potential benefits for use in clinical 3D gel dosimetry without the need for the complicated  $B_1$  field correction method.

**ACKNOWLEDGEMENT:** This study was supported by the program of Basic Atomic Energy Research Institute (BAERI) (2009-0078390) and a grant (2012-007883) from the Mid-career Researcher Program funded by the Ministry of Education, Science & Technology (MEST) of Korea. **REFERENCES:** [1] De Deene Y et al., Phys Med Biol (2000) [2] Willinek WA et al., Radiology (2010) [3] Baldock C et al. Phys Med Biol (2001) [4] Cunningham C et al., Magn Reson Med (2006)

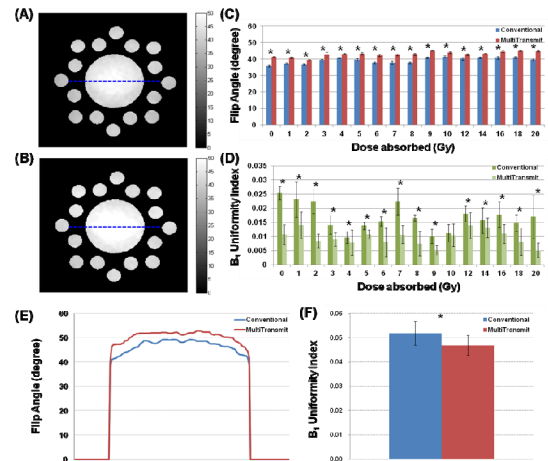


Fig.1. Comparison of  $B_1$  field map between conventional single-source (A) and MultiTransmit imaging (B). (C, E) The flip angle (D, F)  $B_1$  uniformity index measured on ROI placed on calibration vial and large phantom, respectively are shown.

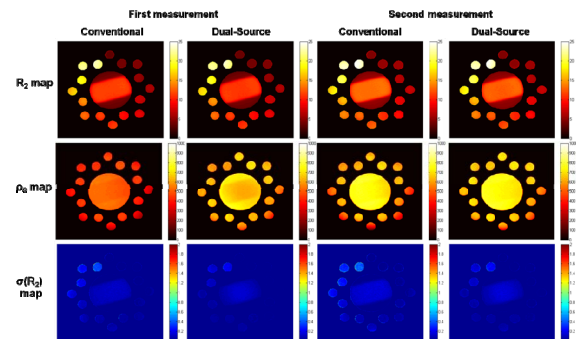


Fig. 2. Spatial and temporal variations of  $R_2$  map and corresponding  $\rho_0$ ,  $\sigma(R_2)$  map. The doses for the calibration vials were 0 to 10 Gy with 1 Gy step, and 12 Gy to 20 Gy with 2 Gy steps (from top center : clockwise).

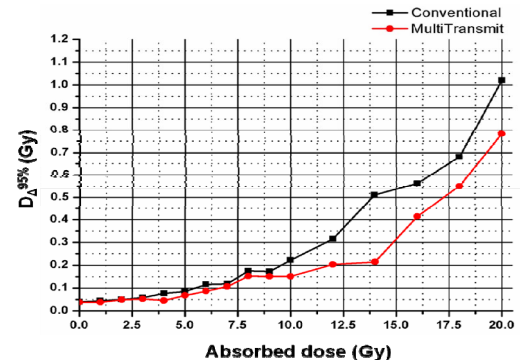


Fig.3. Comparison of dose resolution for BANG3 gel dosimeter between both measurement methods.